



Synthesis and application of biochar from agricultural by-products. Effect of pyrolysis temperature on the acid-base properties of biochar

Phung Thi Lan^{1*}, Vu Tran The Hien¹, Phan Đình Khanh Nguyen², Le Minh Cam^{1,3}

¹ Faculty of Chemistry, Hanoi National University of Education, 136 Xuan Thuy, Cau Giay, Hanoi, Vietnam

² Faculty of Chemistry, College of Education, Vinh University, 182 Le Duan, Vinh, Nghe An, Vietnam

³ Thanh Do University QL 32, Kim Chung, Hoai Duc, Ha Noi, Vietnam

*Email: lanpt@hnue.edu.vn

ARTICLE INFO

Received: 01/4/2024

Accepted: 08/5/2024

Published: 30/06/2024

Keywords:

Biochar, agriculture by product, pyrolysis methylene Blue, adsorption kinetics,

ABSTRACT

Biochar was synthesized from banana peels using the pyrolysis method in a nitrogen gas environment. The pyrolysis temperature ranged from 100°C to 500°C with a heating rate of 5°C per minute and a pyrolysis time of 1.5 hours. The influence of the pyrolysis temperature on the acid-base properties of the biochar surface was evaluated through characteristic SEM and BET measurements. Boehm titration showed a gradual decrease in the total acid functional groups and an increase in the total base functional groups with the increasing pyrolysis temperature. Methylene Blue (MB) was used as a model substance to investigate the adsorption properties of the synthesized biochar. The Langmuir and Freundlich models were employed to describe the adsorption equilibrium. The kinetics of MB adsorption followed a pseudo-second-order kinetic equation. The adsorption capacity of MB by biological charcoal was influenced by the acid-base properties of the material, indicating the impact of the pyrolysis temperature.

1. Introduction

The environmental crisis has motivated researchers to search for new green, friendly strategies to enhance resources [1]. Biochar is a carbon-rich product obtained by decomposing organic matter under thermal conditions with a limited supply of oxygen. Currently, most raw materials for biochar production are agricultural and forestry solid waste, sewage sludge, and other organic solid waste [2]. As a result, biochar preparation itself is a process of recycling organic waste with many benefits: waste treatment, environmental protection, and reducing biochar treatment costs [3, 4]. However, the physical and chemical changes that occur during the synthesis of biochar are complex and depend on both the nature of the biomass and the pyrolysis conditions. These conditions and the

properties of the raw material (composition, particle size distribution, and pore size, among others) largely determine the properties of biochar [6].

Potential applications of biochar include as an energy source (biofuel), soil conditioner, and adsorbent [7, 8]. As an adsorbent, the application of biochar is expected to increase in the near future and may be considered as viable cost-effective substitute for activated carbon [9 - 12].

Our most recent research, focuses on the synthesis of biochar from banana peels, a source of agricultural by products, which are composites of aliphatic and aromatic groups and having abundant functional groups such as hydroxyl, epoxy, carboxyl, carbonyl, ether, ester, amide, sulfonic, and acyl groups as well as

minerals and trace metals [13]. During the heating process, nitrogen-containing functional groups were generating. In a comparative study of nitrogen-doped biochar with one derived from phosphoric acid activation for the removal of an azo dye, acid red 18, L. Wang et al. [14] concluded that maximum adsorption capacity increased by 40% due to the beneficial effect of N-functional. The temperature during the pyrolysis of biochar is the most important factor affecting the surface area, pH, carbon content, surface charge, stability, volatile fraction, and other physicochemical properties [13].

The objective of this work is to investigate in the impact of pyrolysis temperature, one of the important variables in the biochar production process, on the porosity and acid-base properties of the synthesized biochar. The effect of pyrolysis temperatures on the remediation of colored organic wastewater using methylene blue (MB) as a prober was also discussed. The adsorption equilibrium and adsorption kinetics were investigated in detail.

2. Experiments

Preparation of biochar from banana peels

Banana peels were washed, dried in the air, and dried further in a convectional oven at 60°C to a constant weight. The obtained sample was denoted as VCK. After that, VCK was pyrolyzed in an N₂ atmosphere at five different temperatures: 100°C, 200°C, 300°C, 400°C, and 500°C. The heating rate was 5°C.min⁻¹. Pyrolysis time was 1.5 hours. The biochar samples after pyrolysis were labeled TSH-VC100, TSH-VC200, TSH-VC300, TSH-VC400, and TSH-VC500.

Characterizations

XRF was measured at Vilas 003 – Inspection Center for Building Materials (VIBM) to determine the chemical composition of raw banana peels; SEM images to determine the morphology of the surface; the material samples were captured using an S-4800 device (Hitachi). The specific surface area and pore characteristics were measured using a Tristar 3000 instrument (Micromeritics).

Boehm titration for determining surface functional groups

0.5g of synthesized biochar was added to 50 mL NaOH 0.02N and HCl 0.02N solutions respectively. Next, the mixtures were shaken at room temperature for 24 hours to allow the neutralization reaction to occur completely. After that, the mixtures were filtered.

and titrated with 0.02 N HCl and 0.02 N NaOH solutions to determine the total acid and base content.

Determination of the pH of zero charge point (pH_{pzc})

The procedure for determining the pH_{pzc} consisted of adding 0.1 g biochar in 50 ml of 0.1 M NaCl solution in different conditions of starting pH, ranging from 3 to 11 (pH_i). Then, adsorption was maintained for 60 minutes at room temperature under 150 rpm shaking. The solutions were filtered and the final pH of the solution was determined. Plot $\Delta\text{pH} = \text{pH}_f - \text{pH}_i$ vs. pH_i. The pH_{pzc} is the intersection of the graph with the horizontal axis corresponding to $\Delta\text{pH} = 0$.

Bath adsorption experiments of MB by biochar

Adsorption isotherms

0.25 mg of synthesized biochar samples were added into six erlenmeyers already containing 50 mL of MB solution at different initial concentrations (C₀): 30, 40, 50, 60, 70, and 80 mg/L. The mixtures were under agitation of 150 rpm for 24 hours at room temperature.

Kinetics of adsorption

In the experiment, 200 mL MB 80 mg/L solution was utilized to examine adsorption kinetics. 1.0 g of synthesized material was added in the MB solution. The solution was shaken at 150 rpm. The adsorption process takes 180 minutes in total. Every 15 min 3.0 mL samples were collected for MB analysis. The MB concentration was determined by UV-vis spectroscopy. The I absorbance was measured at the maximum wavelength of 664 nm. All adsorption experiments were conducted at the pH of the MB solution without pH adjustment unless otherwise specified.

3. Results and discussion

Characterization results

Chemical composition analysis of raw banana peels by XRF indicated that the collected banana peel has a high carbon content (> 90%), a low ash (solid) content, and certain minerals (6.8% K₂O; 0.82% CaO; 0.12%MgO; 0.2%P₂O₅; 0.02% Fe₂O₃).

The presence of bonds in the aromatic ring on the surface of TSH-VC was verified by FT-IR spectrum (Fig 1, the IR spectrum of a raw banana peel provided for comparison). Almost no characteristic peaks of functional groups containing oxygen are visible. The stretching vibration of O-H bond is represented by a peak at about 3444 cm⁻¹. The saturated CH₂ bond's stretching vibration is indicated by a peak at 2920.2

cm^{-1} , and the spectral pattern at 1627.9 cm^{-1} is assigned to the vibration of the C=C group in the aromatic ring.

The characteristic peak at roughly 1022.3 cm^{-1} is responsible for the vibration of >C-O- in the aromatic ring (OH group in the C-OH bond of phenol). The C=O vibrations of the carboxyl -COOH group are characterized by a peak approximately 1720 cm^{-1} , but they were absent in the spectrum of TSH.

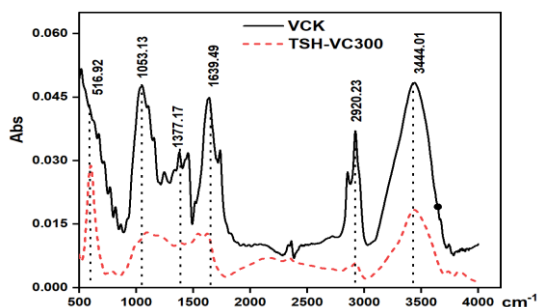


Fig. 1: FT-IR spectra of biochar (TSH-VC300) and of raw banana peel (VCK)

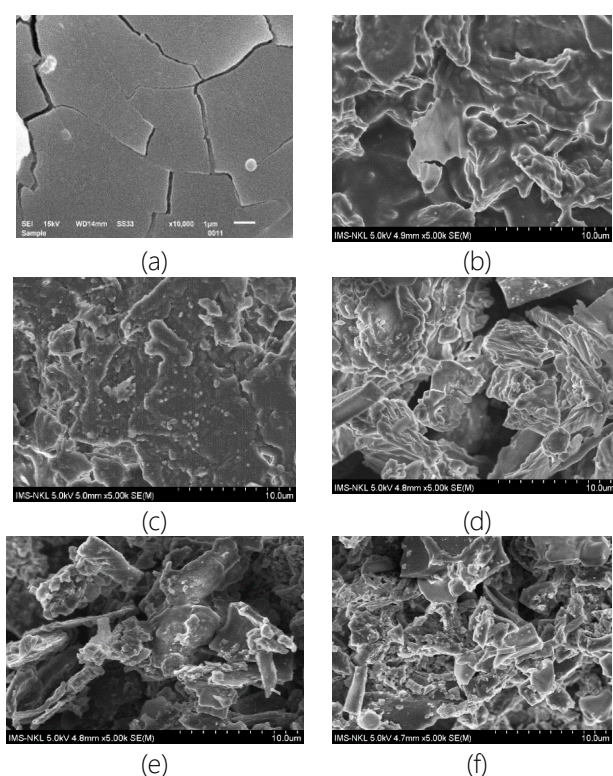


Fig 2: SEM images of VCK (a), TSH -VC100 (b), TSH -VC200 (c), TSH -VC300 (d), TSH -VC400 (e) and TSH -VC500 (f)

The morphology of raw banana peel was determined by SEM images (Fig 2 a). Fig 2 b, c, d, e, and f illustrate the morphology of synthesized biochars at five different pyrolysis temperatures. It can be seen that raw banana peels are devoid of porosity, during pyrolysis, the cavities and porosity were generated and

the porosity gradually increased as the pyrolysis temperature increased. The N_2 adsorption and desorption isotherms measurements revealed that, the specific surface areas of biochar synthesized from banana peels are quite small; but the surface area and the cavities develop as pyrolysis temperatures increase from 100°C to 500°C . (Table 1).

Table 1: The textures of the synthesized Biochars

Sample	S (m^2/g)	V (cm^3/g)	D (nm)
TSH-VC 100	1	0.002	5.127
TSH-VC 200	3	0.003	5.087
TSH-VC 300	3	0.004	5.896
TSH-VC 400	6	0.014	11.582
TSH-VC 500	4	0.015	16.694

Note: S: Specific surface area, V: Total pore volume, D: pore diameter

Determination of pH_{pzc}

The pH of zero charge point of TSH was determined between the pH range of 3 to 11. The plots of ΔpH as a function of pH prior to adsorption. The experimental results showed that the pH_{pzc} of TSH samples increased as the pyrolysis temperature increased. As the pyrolysis temperature is 100°C , the pH_{pzc} was determined to be 5.6. The TSH-VC200 sample has a pH_{pzc} of 6.5. At pyrolysis temperature of 300°C , TSH-VC300 showed a pH_{pzc} of 6.7. When the pyrolysis temperature increased to 400°C , the pH_{pzc} of sample was 8.1 and it was elevated to 8.7 for TSH-VC500. At pH values upper pH_{pzc} , the surface possess negative charge density. Thus to enhance the electrostatic attraction between TSH-VC and MB (cationic dye) the MB adsorption need to conduct at a pH that is higher than pH_{pzc} .

Boehm Titration

The approximate identification of acid and basic functional groups on the surface of TSH-VC was possible via Boehm titration. The obtained results demonstrated that: as the pyrolysis temperature gets higher the total number of acid functional groups on the surface progressively decreased from 1,64 mmol/g for TSH-VC100 down to 0.49 mmol/g in TSH-VC500 samples. Whereas the total amount of basic functional groups gradually increased from 0.33 mmol/g in TSH-VC100 upto 2.25 mmol/g in TSH-VC500 samples.

The effect of pyrolytic temperature on the properties of synthesized biochars

Our finding are in good agrrement with published works [15-16]. Zheng et al. [16] demonstrated that with

increased pyrolysis temperature the polarity of biochar decreases, hence, the hydrophilicity of the biochar surface decreases. Biochar produced at low temperature has a high acidity, polarity, low aromatic content. With an increase in the process temperature, acid function groups (e.g. –OH and –COOH) and the biochar yield decrease, that is, the alkaline functional groups, pH, ash content in biochar increase. The surface area of biochar also increases with the release of volatiles from biomass. Regardless of the type of raw material used, the development of a biochar microstructure and the increased surface area have been widely observed with an increased pyrolysis temperature [17].

Adsorption of MB by TSH-VC samples

Adsorption Isotherms

The equilibrium adsorption capacity (q_e , mg/g) was calculated according to formula (1):

$$q_e = \frac{(C_o - C_e)V}{m} \quad (1)$$

Where C_o (mg/L) and C_e is the initial concentration (mg/L) and the equilibrium concentration of MB, respectively; V (L) is the volume of MB solution, m (g) is the mass of biochar, and q_e (mg/g) is the adsorbed amount at the equilibrium.

Fig 3A presents the adsorption capacity (q_e , mg/g) as a function of the equilibrium concentration (C_e , mg/L) for five biochar samples. It is evident that biochars possess a high effective MB adsorption capability, but, the temperature of pyrolysis strongly influence on the MB adsorption capacity of biochars.

The adsorption equilibrium data were analyzed using two isotherm adsorption models. Langmuir model (2):

$$\frac{C_e}{q_e} = \frac{1}{q_{max}} C_e + \frac{1}{K_L q_{max}} \quad (2)$$

and Freundlich model (3): $\ln q_e = \ln K_F + \frac{1}{n} \ln C_e$ (3)

Where q_{max} (mg/g) is the maximum adsorption capacity; K_L is adsorbate/adsorbent interaction constant (L/mg); K_F is a measure of adsorbent capacity and slope $1/n$ is the adsorption intensity.

Fig 3B and 3C show that MB adsorption by biochars followed both the Langmuir (Fig 3B) and Freundlich (Fig 3C) isotherm models; However, the Langmuir model fits the data better as indicated by the value of the regression coefficient R^2 (Table 2) demonstrating the formation of monolayer interaction action between adsorbent and adsorbate. Table 2 show parameters of both model in different pyrolysis temperatures. The

q_{max} and K_L values firstly increased gradually with increasing pyrolysis temperature from 100°C and achieved their maximum values at 300°C. As the pyrolysis temperature further increasing to 400°C and 500°C the adsorption capacity, however, decreased. The K_F and $1/n$ represent the Freundlich constants. The pyrolysis temperature –induced changes of K_F and $1/n$ values were similar to those of Langmuir parameters. The parameter $1/n$ was interval from 0 to 1, suggesting that the MB adsorption onto TSH-VC was favorable and also that there were minimum interaction between the adsorbed molecules [18].

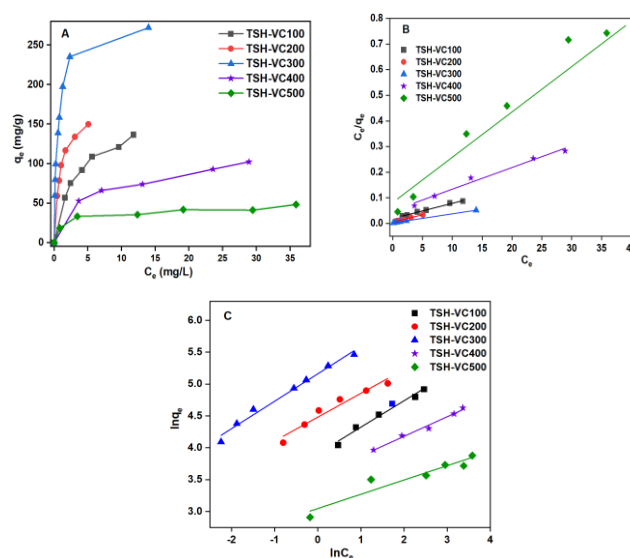


Fig 3: Equilibrium adsorption of MB by TSH-VCs: Equilibrium adsorption of MB onto different TSH-VC samples (A); Langmuir (B) and Freundlich (C) isotherm models for MB adsorption by f different TSH-VC samples

The obtained results in this work are in good agreement with the work done by Liu S. et al. [19] who studied the adsorption capability of banana pseudostem biochar towards MB at low temperature. It was worthy noted that the presence of N-containing groups could be favourable for adsorption of MB [20]. The adsorption capability of the biochar can comparative with activated carbon, however the synthesis of biochar is much more easier. For example, An MB adsorption capability of 5.88 mg g⁻¹ on activated carbon obtained from grape wood wastes has been reported by Mousavi et al. [21]. AC modified by anionic surfactants presented a maximum adsorption capacity of MB obtained by the Langmuir model is 232.5 mg g⁻¹ [22]. El-Bery et. al [23] reported the fabrication of activated carbon derived from lignocellulosic wastes ($S_{BET} = 2490$ m²g⁻¹), and an MB adsorption capacity of 148.8 mg g⁻¹ was observed. The

maximum adsorption capacity of 322 mg g⁻¹ of the activated carbon made from Rumex abyssinicus plant was recorded in the study of Fito et. al. [24].

Table 2: The parameters of Langmuir and Freundlich adsorption isotherm models.

	K _L	q _{max} (mg/g)	R ²	K _F	n	R ²
TSH - VC 100	0.31	169.49	0.992	49.82	2.41	0.974
TSH - VC 200	1.16	175.44	0.999	88.23	2.67	0.945
TSH - VC 300	2.93	277.78	0.985	180.31	2.20	0.984
TSH - VC 400	0.17	117.65	0.982	35.28	3.25	0.984
TSH - VC 500	0.41	47.85	0.980	21.03	4.46	0.910

Kinetics of adsorption

Fig. 4A shows the effect of the contact time for MB adsorption on synthesized biochars as a function of different pyrolysis temperatures. The removal of MB increased rapidly during the initial MB adsorption stages due to the sites available for sorption on the surface. However, with increasing surface coverage, the number of remaining binding sites decreased dowing to the repulsive forces between the adsorbed and free molecules, leading to the equilibrium state being achieved [25]. Two kinetic models of Pseudo First-Order (Eq. 4) and Pseudo Second-Order (Eq. 5) were considered to investigate the mechanism of MB adsorption. Linear kinetic models were compared using the R² values as reference.

$$\ln(q_e - q_t) = \ln q_e + k_1 * t \quad (4)$$

$$\frac{t}{q_t} = \frac{1}{q_e} * t + \frac{1}{k_2 q_e^2} \quad (5)$$

Where q_t (mg/g), q_e (mg/g) are the amounts of MB adsorbed at time t in min and at equilibrium, respectively; k₁ and k₂ are the pseudo first order rate constant (min⁻¹) and second order rate constant (g mg⁻¹ min⁻¹), respectively. According to the linear fitted plots presented in Fig 4B and 4C, the MB adsorption kinetics on TSH-VC samples were inconsistent with Pseudo First-Order kinetic model. The obtained rate constants k₁ × 10² (min⁻¹) for TSH-VC100, TSH-VC200, TSH-VC300, TSH-VC400 and TSH-VC500 were 1.38, 1.93, 3.19, 3.30 and 0.05 respectively. However, the correlation coefficients were much smaller than 1. The

experimental data closely resemble Pseudo-Second-Order kinetic model with the rate constants k₂ (g mg⁻¹ min⁻¹) of 0.00053, 0.00066, 0.00247, 0.1100 and 0.5800 for TSH-VC100, TSH-VC200, TSH-VC300, TSH-VC400 and TSH-VC500 samples respectively, and the correlation coefficients are approximately 1.

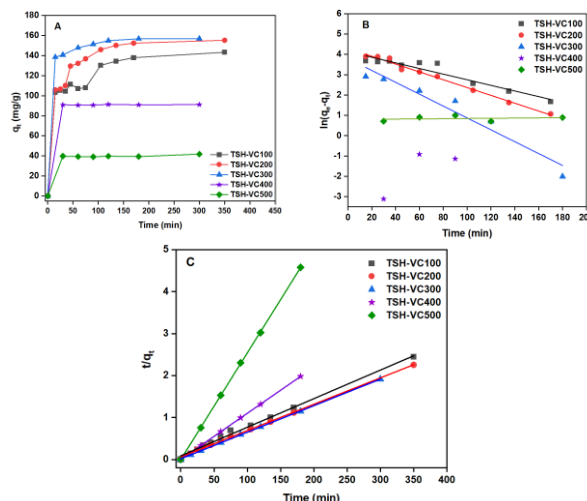


Fig 4: Kinetics of adsorption of MB onto TSH-VC Amount of MB adsorption (q_t) as a function of time onto different TSH-VC (A); Pseudo First-Order (B) and Pseudo-Second-Order (C) kinetic models for MB by different TSH-VC samples

Effect of pyrolysis temperatures on the MB adsorption by the as-prepared biochar

The obtained experimental results demonstrated that as-synthesized biochars exhibited a good MB adsorption ability even though only thermally decomposed and didn't require any process of activation. However, the MB adsorption capacity increased gradually from TSH-VC100 to TSH-VC300 and reaches a maximum at the thermal decomposition temperature of 300°C, then decreased gradually when TSH was thermally decomposed at 400°C and at 500°C. This trend can be explained by reasons: 1) MB is a cationic dye, so it has strong affinity with the base surface. The results of Boehm titration showed that as the pyrolysis temperature increases, the surface acid property of TSH decreases gradually while the surface base property increases. Therefore The MB adsorption capacity of TSH-VC increase. 2). According to Boehm titration, TSH-VC400 and TSH-VC500 possess a highest surface base property, their adsorption capacity of MB however, were lower compared to TSH-VC 300 (Table 2). This is explained by the fact that, besides the acid-base nature of the surface, the MB adsorption capability also depends on the pH_{pzc}. The presence

of negatively charged functional groups on the adsorbent surface is necessary for the adsorption of the basic dye [21]. All MB adsorption experiments in this work were conducted at a pH of 6.3, which is self-generated pH. This value is close to the pH_{pzc} values of TSH-VC 200 and TSH-VC 300, while the pH_{pzc} values of TSH-VC 400 and TSH-VC 500 are both greater than 8.0. Therefore, the increasing trend in MB adsorption capacity up to a maximum at TSH-VC 300 and then decreased at TSH-VC 400 and TSH-VC 500 can be explained.

4. Conclusion

In this study, Biochars was synthesized from banana peels by pyrolysis at different temperatures under a nitrogen atmosphere. The influence of pyrolysis temperature on the properties of biochar was evaluated through SEM images and the BET method. The obtained results demonstrated that the porosity of the biochar surface gradually increased with increasing pyrolysis temperatures and begins to have cavities. The Boehm titrations suggested that as pyrolysis temperature increased gradually increased the basicity and gradually decreased the acidity of the surface. The pH_{pzc} of synthesized biochar samples changed with temperature of pyrolysis process. The adsorption of MB dye by synthesized biochars was investigated, and the results showed that as-prepared biochar has a good adsorption ability of MB dye. The adsorption capacity strongly depends on the acid-base nature of the material surface; that is, it depends on the pyrolysis temperature and is less affected by the porous nature of the material surface. In accordance with experimental results, biochar exhibited the highest capability to adsorb MB with a maximum adsorption capacity of 277.78 mg/g, is one was thermally decomposition at the temperature of 300°C. The study's results demonstrated that biochars synthesized from banana peels solely by pyrolysis possess a good capacity to adsorb organic dyes. TSH-VC may be applied as an effective and affordable adsorbent.

References

1. B. Ahmad, V. Yadav, A. Yadav, M.U. Rahman, W.Z Yuan, Z. Li, X. Wang, *Sci. Total Environ.* 719 (2020) 137315. <https://doi.org/10.1016/j.scitotenv.2020.137315>
2. X. Xiao, B. Chen, Z. Chen, L. Zhu, J.L. Schnoor, *Environ. Sci. Technol.* 52 (2018) 5027–5047. <https://doi.org/10.1021/acs.est.7b06487>
3. A. F. Sanromán, M. Pazos, E. Rosales, M. A. Sanromán, *Appl. Sci.* 10 (2020) 7810. <https://doi.org/10.3390/app10217810>
4. N. Cheng, B. Wang, B. Wu, X. Lee, Y. Xing, M. Chen, B. Gao, *Environ. Pollut.* 273 (2021) 116448. <https://doi.org/10.1016/j.envpol.2021.116448>
5. T. D. Minh, J. Song, A. Deb, L. Cha, V. Srivastava, M. Sillanpää, *Chem. Eng. J.* 394 (2020) 124856. <https://doi.org/10.1016/j.cej.2020.124856>
6. C. Zhang, Z. Zhang, L. Zhang, Q. Li, C. Li, G. Chen, S. Zhang, Q. Liu, X. Hu, *Technol.* 304 (2020) 123002. <https://doi.org/10.1016/j.biortech.2020.123002>
7. F. R. Oliveira, A. K. Patel, D.P. Jaisi, S. Adhikari, H. Lu, S. K. Khanal, *Bioresour. Technol.* 246 (2017) 110e122. <https://doi.org/10.1016/j.biortech.2017.08.122>
8. B. Wang, B. Gao, J. Fang, *Crit. Rev. Environ. Sci. Technol.* 47 (2017) 2158e2207. <https://doi.org/10.1080/10643389.2017.1418580>
9. R. Li, Y. Zhang, H. Deng, Z. Zhang, J.J. Wang, S.M. Shaheen, R. Xiao, J. Rinkebe, B. Xi, X. He, J. Du, *J. Hazard Mater.* 384 (2020), 121095. <https://doi.org/10.1016/j.jhazmat.2019.121095>
10. P. Krasucka, B. Pan, Y. Sik Ok, D. Mohan, B. Sarkar, P. Oleszczuk, *Chem. Eng. J.* 405 (2021) 126926. <https://doi.org/10.1016/j.cej.2020.126926>
11. M. B. Ahmed, J.L. Zhou, H.N. Ngo, W. Guo, *Biomass Bioenergy* 84 (2016) 76 - 86. <https://doi.org/10.1016/j.biombioe.2015.11.002>
12. C. Keske, T. Godfrey, D.L.K. Hoag, J. Abedin, *Food Energy Secur.* 9 (2020) e188. <https://doi.org/10.1002/fes3.188>
13. Y. Li, B. Xing, Y. Ding, X. Han, S. Wang, *Bioreour. Technol.*, 312 (2020), 123614. <https://doi.org/10.1016/j.biortech>,
14. L.Wang, W. Yan, C. He, H. Wen, Z.Cai, Z. Wang, Z. Chen, W. Liu, *Appl. Surf. Sci.* 433 (2018) 222 - 231. <http://dx.doi.org/10.1016/j.apsusc.2017.10.031>
15. X. Zhang, P. Zhang, X. Yuan, Y. Li, L. Han, *Bioresour. Technol.* 296 (2020) 122318. <https://doi.org/10.1016/j.biortech.2019.122318>
16. X. Zheng, Y. Zhou, X. Liu, X. Fu, H. Peng, S. Lv, *Bioresour. Technol.* 297 (2020) 122413, 2020]. <https://doi.org/10.1016/j.biortech.2019.122413>
17. J. Li, Z. Liu, Y. Tian, Y. Zhu, S. Qin, Y. Qiao, *Bioresour. Technol.* 304 (2020) 122735 <https://doi.org/10.1016/j.biortech.2020.122735>
18. J. S. Calisto, I. S. Pacheco, L. L. Freitas, L. K. Santana, W. S. Fagundes, F. A. Amaral, S. C. Canobre, *Heliyon* 5 (2019). 6;5(12):e02553. <https://doi.org/10.1016/j.heliyon.2019.e02553>
19. S. Liu, J. Li, S. Xu, M. Wang, Y. Zhang, X. Xue, *Bioresour. Technol.* 282 (2019) 48–55. <https://doi.org/10.1016/j.biortech.2019.02.092>
20. M. Mian, and G. Liu, *Chemosphere* 215 (2019) 101-104. <https://doi.org/10.1016/j.chemosphere.2018.10.027>
21. S. Al. Mousavi, D. Shahbazi, A. Mahmoudi and P. Darvishi, *Water Qual. Res. J.* 57 (1) (2021) 1 - 19. <https://doi.org/10.2166/wqrj.2021.015>
22. Y. Kuang, X. Zhang, S. Zhou, *Water* 12(2) (2020) 587. <http://doi.org/10.3390/w12020587>
23. H. M. El-Bery, M. Saleh, R. A. El-Gendy, M. R. Saleh, S. M. Thabet, *Scientific Reports* (2022) 12:5499. <http://doi.org/10.1038/s41598-022-0945-4>
24. J. Fito, M. Abewaa, A. Mengistu, *Sci. Rep.* 13 9 (2023), 5427. <https://doi.org/10.1038/s41598-023-32341-w>
25. S. Yu, Y. Liu, Y. Ai, X. Wang, R. Zhang, Z. Chen, Z. Chen, G. Zhao, X. Wang, *Env. Pollut.* 242 part A (2018) 1-11. <https://doi.org/10.1016/j.envpol.2018.06.031>